Design and Validation of a GPS Logger System for Recording Aerially Deployed Herbicide Ballistic Technology Operations

Roberto Rodriguez, III, *Student Member, IEEE*, Daniel M. Jenkins, and James J. K. Leary

***Abstract*— Herbicide ballistic technology (HBT) is an electro-pneumatic delivery system designed for administering 17.3-mm herbicide-filled projectiles (e.g., paintballs) to visually acquired weed targets. Currently, HBT is being deployed from a Hughes 500D helicopter platform in aerial surveillance operations to eliminate satellite invasive weed populations in remote natural watershed areas of Maui (HI, USA). In an effort to improve operations, we have integrated GPS and other sensor hardware into the electropneumatic device for instantaneous recording of time, origin, and trajectory of each projectile discharged by the applicator. These data are transmitted wirelessly to a custom android application that displays target information in real time both textually and graphically on a map.**

***Index Terms*— Data acquisition, geospatial analysis, global positioning system, sensor integration and fusion.**

I. Introduction

INVASIVE, exotic plant species are threatening the endemic biological integrity of the Hawaiian archipelago [1]–[7]. Moreover, the islands' extreme topography and dense vegetation are an impediment to effective mitigation [8]. Herbicide Ballistic Technology (HBT) is a concept to address these challenges with a novel capability to treat invasive plant targets with long-range accuracy [9]. In previous implementations, the HBT platform enhances helicopter surveillance operations with the capability of eliminating high-risk satellite populations of invasive plant targets, which are occupying remote inaccessible areas of watershed [10].

II. Background

The HBT platform is an herbicide delivery system currently registered in the state of Hawaii as a Special Local Need pesticide for treating nascent miconia (*Miconia calvescens* DC) and strawberry guava (*Psidium cattleianum*) patches in remote natural areas [9]. The basic concept of HBT is the encapsulation of an active herbicide formulation into 17.3 mm soft-gel projectiles (i.e., paintballs) for accurate, long-range delivery to weed target via propulsion from an electro-pneumatic marker. Projectiles can be delivered to a target with an estimated effective range of ∼30m, presenting novel opportunities for managing areas with extreme, inaccessible landscapes (e.g., ravines and cliff faces).

The adoption of satellite navigation (utilizing GPS and GLONASS) in HBT operations has allowed for the acquisition of large data sets leading to explicit spatial and temporal performance evaluation of an operation [10]. Current op erational procedures call for reference points to be recorded for each target treated using a consumer-grade GPS receiver capturing latitude, longitude, elevation and timestamp. At the end of each operation, the applicator also records the estimated total consumption of projectiles that is later translated into the average dose rate for the total targets treated in that operation.

Attitude and heading reference systems (AHRS) provide the roll, pitch and yaw of a body and are commonly used for navigation purposes. Recent development in micro-electro-mechanical systems (MEMS) based AHRS systems are being used in a number of applications, including unmanned aerial vehicles (UAV) [11], commercial airplanes [12], along with terrestrial [13] and submerged navigation [14]. However, many of these systems have a large profile and require wired connections to data recording devices making them ill suited for implementation with the HBT platform.

To enhance operational data acquisition, a custom, prototype HBT-Logging System (HBT-LS) was developed for integration with the electro-pneumatic marker automating data acquisition for every projectile discharged. Data acquired includes the above mentioned spatial and temporal assignments, along with added attributes for tilt and azimuth of the marker position (Fig. 1). New analyses of HBT-LS data sets include: (i) accurate accounts of projectile dose rates assigned to each target, (ii) the time to deliver projectile dose to target and (iii) offset projections of the actual target location.

Here in, we report on the basic hardware and software specifications of HBT-LS with static and dynamic calibrations in controlled and operational settings, respectively. This includes a discussion on improvements in the data management process and technology limitations requiring further development.

Manuscript received September 15, 2014; revised November 3, 2014; accepted November 11, 2014. Date of publication November 20, 2014; date of current version January 29, 2015. This work was supported in part by the U.S. Department of Agriculture (USDA) Forest Service, in part by the Special Technology Development Program under Award R5-2012-01 through the Hawaii Department of Land and Natural Resources Forest Health Program, in part by the Hawaii Invasive Species Council under Award POC 40466, in part by the USDA Hatch Act Formula Grant under Project 112H, and in part by the USDA Renewable Resources Extension Act. The associate editor coordinating the review of this paper and approving it for publication was Prof. Octavian Postolache.

R. Rodriguez III and D. M. Jenkins are with the Department of Molecular Bioscience and Biological Engineering, University of Hawaii at Manoa, Honolulu, HI 96822 USA (e-mail: roberto6@hawaii.edu; danielje@hawaii.edu).

J. J. K. Leary is with the Department of Natural Resources and Environmental Management, University of Hawaii at Manoa, Honolulu, HI 96822 USA (e-mail: leary@hawaii.edu).

Color versions of one or more of the figures in this letter are available online at http://ieeexplore.ieee.org.

Digital Object Identifier 10.1109/JSEN.2014.2371896

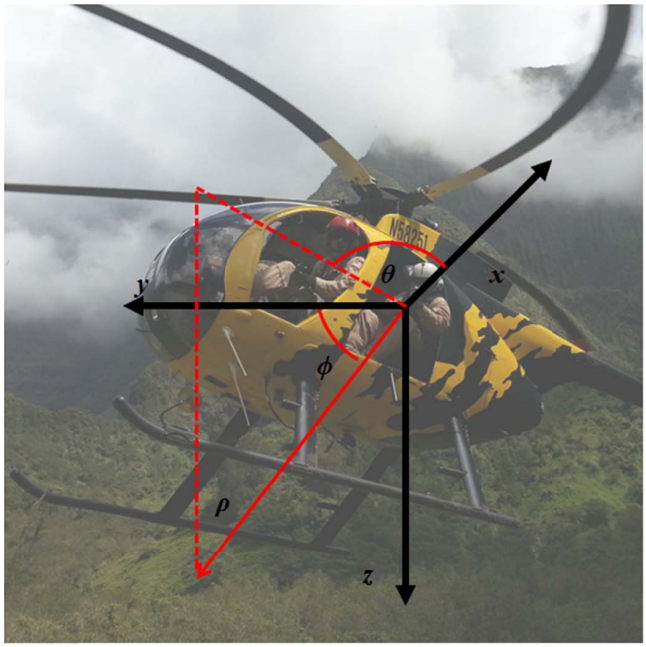

Fig. 1. Spherical coordinate system to describe plant target locations with applicator as the origin.

III. Sensor Development

A. Hardware Design

The relevant data to be recorded include the position (latitude, longitude, and altitude), azimuth and tilt of the marker, depicted in Fig. 1, as well as each discharge of a projectile and the unique target IDs and descriptions of each targeted plant. Latitude and longitude are recorded within a custom Android user interface from the built in GPS chip (Broadcom BCM4751) on the interfacing Android device. Most non-GPS information is recorded on a custom circuit (Fig. 2) with individual sensors communicating to a simple 8-bit microcontroller (ATMEGA328P-MUR, Atmel Corp., San Jose, CA) which transmits data wirelessly to the Android application through a serial Bluetooth module (RN42, Roving Networks, Los Gatos, CA). Altitude is estimated from barometric pressure measurements based on empirical relationships (MPL3115A2, Freescale Semiconductor, Austin TX). Azimuth and tilt are recorded from inertial (MPU-6050, InvenSense, San Jose, CA) and magnetic (LSM303DLHTR, STMicroelectronics, Geneva, Switzerland) sensors as described below. Projectile discharge is identified by an interrupt triggered by the transistor sinking the solenoid current in the marker, and similarly a momentary contact switch triggers an interrupt to indicate acquisition of a new target (for which a new target ID is automatically assigned). Descriptive information for each target is coded by user selection of radio buttons in the Android interface. In our case, descriptions are coded for the developmental stage of the plant with options for "Juvenile" (not yet bearing fruits/seeds), "Mature" (flower/fruit bearing), or "Survivor" (showing sub-lethal symptoms resulting from a previous herbicide application). Description reverts to the default "Juvenile" for each newly engaged target, as these are by far the most commonly encountered plants in our operations to eliminate incipient satellite populations.

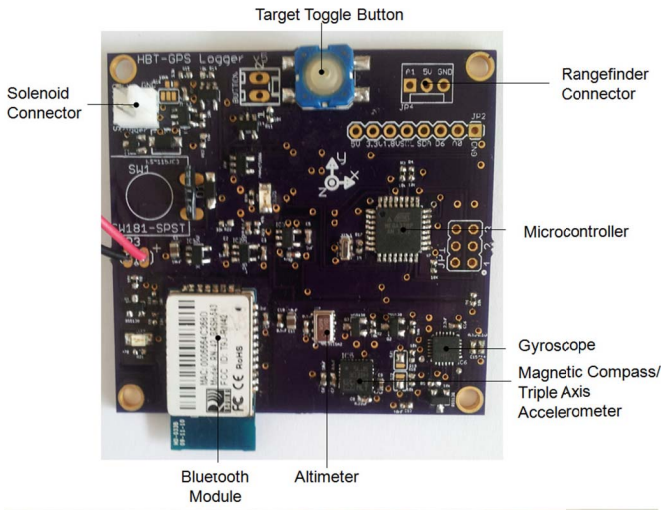

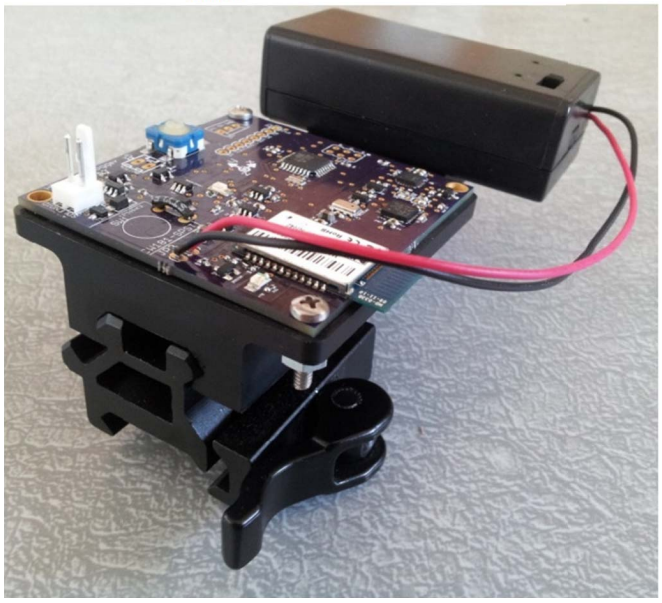

Fig. 2. HBT-Logger System (HBT-LS) with annotations for major components (top), and mounted on rail attachment system (bottom).

1) Altitude: Altitude is automatically inferred from observed barometric pressure (MPL3115A2, Freescale Semiconductor) based on the following internal empirical relationship, by setting the "ALT" bit on Control Register 1 of the sensor:

$$h = 44330.77\left[1 - \left(\frac{p}{p_0}\right)^{0.1902632}\right] + h_{\text{off}} \qquad (1)$$

where h is the height (in meters), p is the pressure (in Pascals), p_0 is the sea level pressure, and h_{off} is the offset in the determined height. To calibrate for variations in barometric pressure, sensors are calibrated at the start of each operation based on the known elevation at the landing site. This known elevation is used by the calibration activity of the Android device to estimate the current sea level pressure based on the current barometric pressure and its empirical relationship with altitude. The new estimate of sea level pressure reference is communicated to the microcontroller and loaded into the "Barometric Pressure Input" Registers of the MPL3115A2.

2) Azimuth and Tilt: The azimuth and tilt, represented by θ and φ in a spherical coordinate system (Fig. 1), are recorded using a triple axis gyroscope/accelerometer (MPU-6050) and a triple-axis tilt-compensated magnetic compass (LSM303DLHTR). Redundant measurements of orientation were made from these devices to facilitate identification and compensation for drift in the azimuth estimated from the gyroscope, or deviations in compass readings resulting from local disturbances in geomagnetic field or interferences by magnetic fields originating from or shielded by the aircraft.

The calibration activity of the Android interface allows the user to overwrite the digitized values stored in device EEPROM corresponding to the maximum and minimum magnetic fields applied in each axis of the compass chip (which vary significantly between devices). This allows the measurements in each axis to be scaled to internally consistent measures of the field strength. This calibration requires the user to align each of 6 reference orientations ($+x$, $-x$, $+y$, $-y$, $+z$, $-z$) of the sensor coordinates with the peak geomagnetic field at the given location. As a result, the 3-D vector of any arbitrary magnetic field is estimated accurately with respect to the marker coordinate system, and vector operations are implemented by the microcontroller to project this vector onto a horizontal plane compensated for tilt and roll of the marker estimated from acceleration measurements on the same chip. These measurements provide an estimate of the orientation of the marker in the horizontal plane with respect to magnetic north. Marker orientation is estimated from the gyroscope readings using custom coded quaternion algebra on the quaternion output retrieved from the digital motion processor of the device using the manufacturer's software library (MotionAppsTM 5.0). The quaternion codes for the current orientation of the sensor with respect to the initial orientation at the startup of the sensor.

Magnetic declination is determined at the start of each operation by orienting the marker along a path aligned with true north (or any other given reference orientation) and communicating this reference orientation to the microcontroller so that the reference with respect to magnetic north can be recorded in EEPROM. On device startup (or recalibration), the marker orientation estimated by the gyroscope, projected onto the horizontal plane, is initialized to the current geographical orientation based on the tilt compensated compass reading corrected for magnetic declination. The marker position (latitude, longitude and altitude), azimuth, and tilt, as depicted in Fig. 1, can be used to infer target position based on overlaying projectile orientation and trajectories onto digital elevation maps, and/or using an estimated range to target, represented by ρ.

3) Trigger Detection: The electro-pneumatic marker discharges projectiles via an actuating solenoid. Projectile discharge is registered by an interrupt caused by a falling edge of this signal, using a custom implemented Schmitt Trigger to prevent multiple interrupts from a single transition and to shift the signal to the microcontroller logic level. The trigger signal is buffered by a voltage follower to prevent loading of the solenoid. In order to prevent triggering from artifacts of resonance in the inductive load associated with the same trigger pull, a latent period is enforced in software during which subsequent falling edges are not registered. This latent period is greater than the period for which oscillations associated with a single projectile discharge occur, but is smaller than the period at which projectiles can be discharged in rapid fire (i.e., >10 projectiles sec^{-1}).

B. Software Design

1) Calculating Plant Target Coordinates: The equations of motion for a spherical projectile travelling in air is [15]

$$m\ddot{\mathbf{r}} = m\dot{\mathbf{v}} = -\frac{1}{2}\rho_A A C_D \left|\vec{\mathbf{v}} - \vec{\mathbf{W}}\right|\left(\vec{\mathbf{v}} - \vec{\mathbf{W}}\right) + \frac{1}{2}\rho_A A C_L \left|\vec{\boldsymbol{v}} - \vec{\boldsymbol{W}}\right|\left[\frac{\vec{\boldsymbol{\omega}} \times \left(\vec{v} - \vec{W}\right)}{\omega}\right] + m\vec{\boldsymbol{g}} \tag{2}$$

where m is the mass of the projectile, $\mathbf{r}$ is the position of the projectile in Cartesian coordinates relative to the origin, $\mathbf{v}$ is the velocity of the projectile relative to the Cartesian coordinate system, ρ_A is the air density, A is the cross-sectional area of the projectile, C_D is the (dimensionless) drag coefficient, $\mathbf{W}$ is the velocity of the wind blowing relative to the same coordinate system, C_L is the (dimensionless) lift coefficient, $\boldsymbol{\omega}$ is the angular velocity of the projectile and $m\boldsymbol{g}$ is the gravitational force. Due to the highly dynamic nature of wind conditions in close proximity to the helicopter, the short range of HBT application, and the relatively large initial velocity of the projectiles, a simplification to linear trajectories is made for real time calculations. However, since all raw data is also recorded more rigorous analysis based on the data is also possible.

The azimuth, tilt, and range describe the location of the target relative to the applicator in a local spherical coordinate system centered at the applicator. In order to superimpose the local coordinates of the target over the geodetic coordinates of the applicator, the local spherical coordinates are converted into local Cartesian coordinates with a North-East-Down reference frame centered at the applicator using the following relationships:

$$x_{A\to T} = \rho \cos\varphi \cos\theta \tag{3}$$

$$y_{A\to T} = \rho \cos\varphi \sin\theta \tag{4}$$

$$z_{A\to T} = \rho \sin\varphi \tag{5}$$

where x, y, and z (with subscript A→T) designate the components of the vector from applicator to target in local Cartesian coordinates and ρ, θ and φ describe the vector in local spherical coordinates. The short range of an HBT application relative to the radius of the Earth allows for simplified calculations using a local flat surface projection. The final target offset coordinates are calculated from the following relationships:

$$\phi_T = \phi_A + \frac{x_{A\to T}}{R_{Earth}} \tag{6}$$

$$\lambda_T = \lambda_A + \frac{y_{A\to T}}{R_{Earth}\cos\phi_A} \tag{7}$$

$$h_T = h_A + z_{A\to T} \tag{8}$$

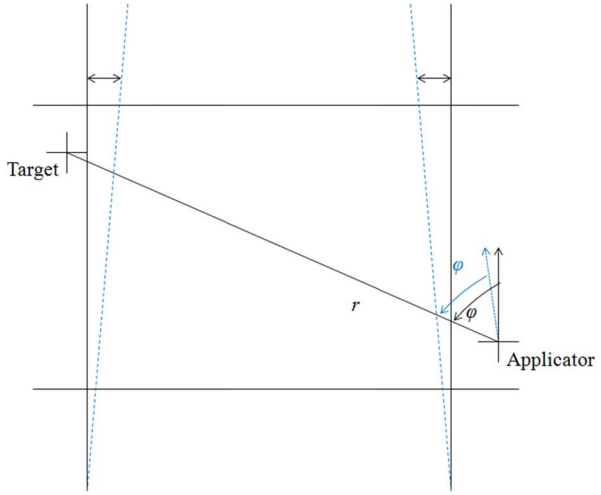

Fig. 3. Errors due to assumptions of flat surface projection (black arrows) include discrepancies of the azimuth and longitude that are dependent on the latitude. Blue dashed lines represent the actual "lines" of constant longitude that converge as latitude increases.

where ϕ, λ and h are geodetic coordinates (with subscripts T for target or A for applicator) and R_{Earth} is the radius of the Earth [16].

The flat surface approximations result in latitude-dependent errors in the estimated values of the azimuth to and longitude of the target (Fig. 3). Using the prefix "Δ" to designate the error in a parameter, errors in the target geodetic coordinates can be estimated from basic uncertainty analysis assuming that errors in each measurement are random and independent:

$$\Delta\phi_T \approx \sqrt{(\Delta\phi_A)^2 + (\xi_\phi(\phi_A))^2} \tag{9}$$

$$\Delta\lambda_T \approx \sqrt{(\Delta\lambda_A)^2 + \left(\xi_\lambda(\phi_A)\right)^2} \tag{10}$$

$$\Delta h_T = \sqrt{(\Delta h_A)^2 + (\Delta\rho\cos\varphi)^2 + (\rho\sin\varphi\,\Delta\varphi)^2} \tag{11}$$

where $\xi(\phi_A)$ is the error due to the flat surface approximation as a function of the applicator's latitude. Due to the short range of the HBT application relative to the radius of the Earth, $\xi(\phi_A)$ is relatively small compared to the horizontal and vertical errors in the GPS receiver. For example, at the approximate latitude of 20.8°, where these tests were conducted, with a range of 30 m and azimuth at 45°, the value of $\xi(\phi_A)$ is less than 10^{-6}° based on comparison with the more rigorous Vincenty formulae using the WGS-84 model, equivalent to about 0.1 m [17].

2) Microcontroller: Machine code was generated using the Arduino IDE (Arduino, Torino, Italy), and programmed onto the microcontrollers (ATMEGA328P-MUR) using software (Atmel Studio 6.1) and programming hardware (AVRISP-mkII) from the manufacturer (Atmel). During normal operation, the microcontroller polls all of the sensors for new data each cycle of the program. Any new data is sent to a paired Google Nexus 7 tablet (Asus Computer International, Fremont, CA) over Bluetooth. Each set of data is preceded by a code uniquely identifying the type of data being sent (i.e. orientation, tilt, altitude, projectile discharge, or acquisition of new target) so that the Android Bluetooth Service can parse the incoming data and update the user interface appropriately.

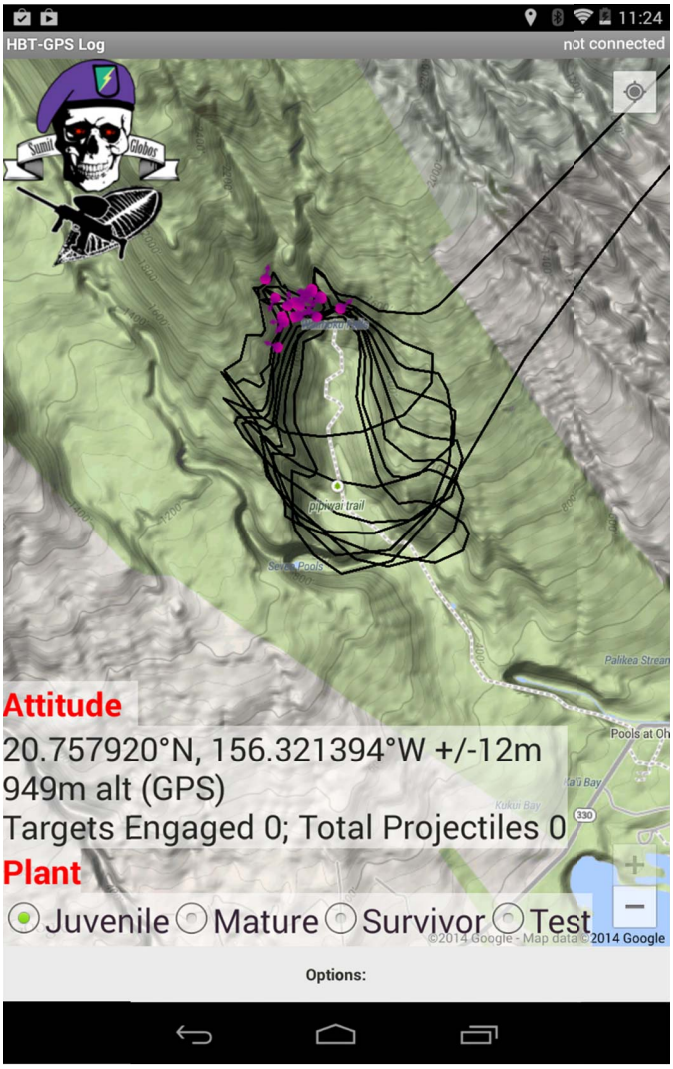

Fig. 4. User interface showing flight path and trajectories of projectiles for a single HBT operation (note that the HBT-LS is not connected so that marker orientation is not displayed, and target and projectile counts are reset to zero). Options available through the options button include connecting or disconnecting to logger over Bluetooth, starting or ending a record of data, e-mailing or displaying recorded data on the map, and launching other activities such as system calibration.

In addition, each batch of data is followed by a custom check code to validate correct transmission of data. Any data that does not contain a valid code and a correct check code is discarded by the Android device without further action. Because data is continuously streamed to the Android device and only the most recent data is recorded to associate with periodic trigger pulls and trackpoints, no attempt to recover incomplete data strings is made.

3) User Interface: An Android device is used to record data, allow the user to send commands (i.e. for calibration) to the microcontroller, and to display device data in real time both textually and on a map (Fig. 4). The custom Android application was developed using the Eclipse IDE to record GPS coordinates, parse incoming Bluetooth data transmitted from the custom hardware, record all data to a comma-delimited file, and update the user interface (with textual and map information) in real-time. An options menu on the main activity interface allows the user to connect

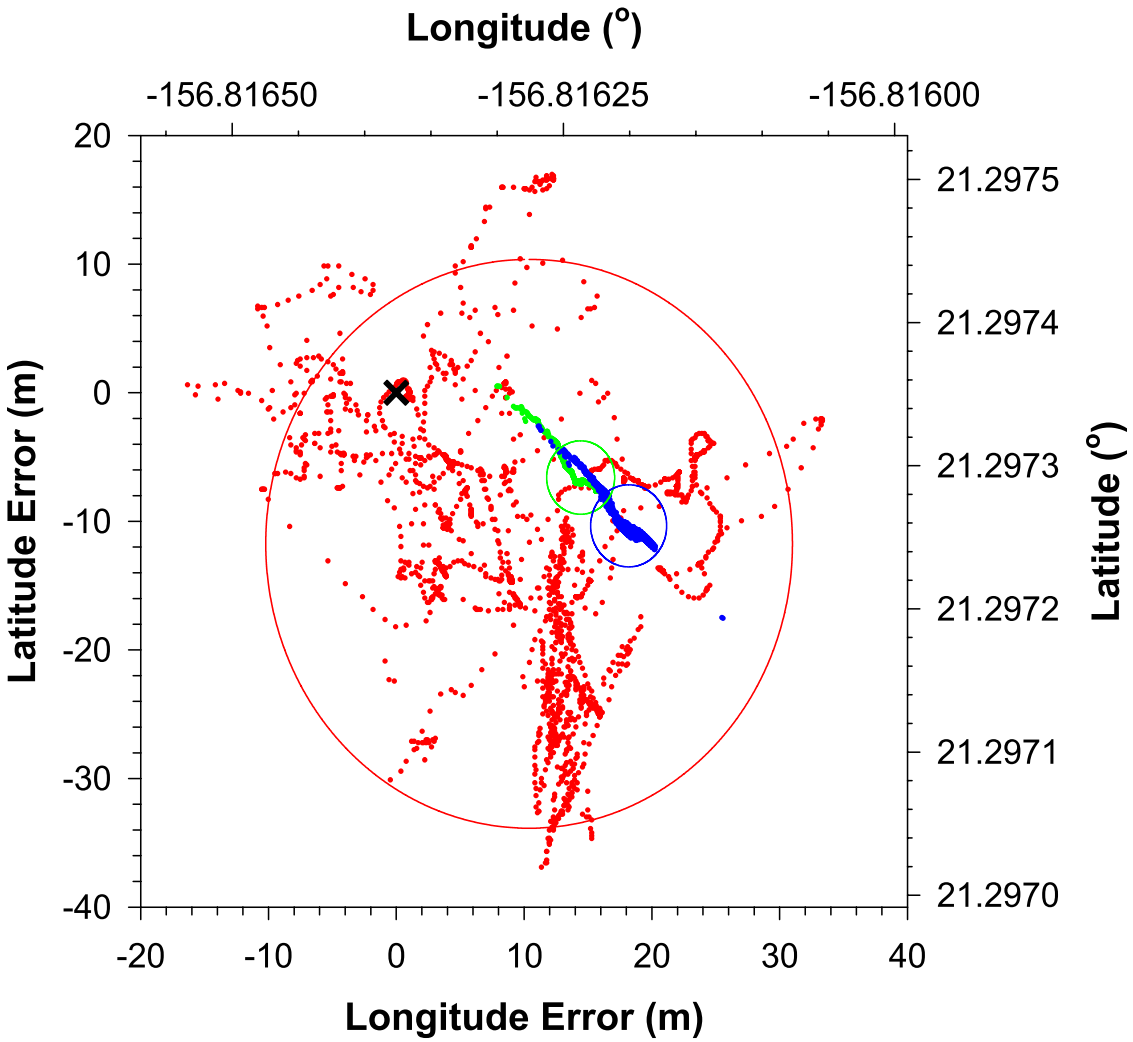

Fig. 5. Predicted locations and associated CMAS for Foretrex 401 (red), Google Nexus 7 (green) and HBT-LS (blue). Reference antenna location is marked with a black X at the origin.

wirelessly to different custom hardware, start and end data logging, display recorded data on the map, or launch other activities such as the calibration options described previously.

IV. Static Accuracy and Precision of HBT-LS

According to the National Standard for Spatial Data Accuracy (NSSDA), the accuracy of a GPS receiver is determined by root mean square error (RMSE), which is the square root of the average of the sum of the squared differences between the coordinate values from a GPS receiver relative to another more accurate source of the same position used as a reference position [18], [19].

Precision of a GPS receiver in the horizontal x and y directions (aligning respectively with lines of constant longitude and latitude), is described by the circular map accuracy standard (CMAS), which is based on the US National Map Accuracy Standards specifying that "no more than 10% of the points in the dataset will exceed a given error" [20]. Therefore, the CMAS is defined as the magnitude of the radius of the smallest circle containing 90% of the recorded positions.

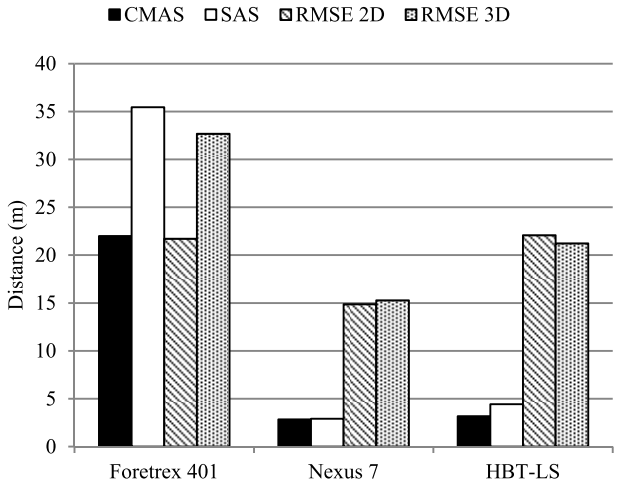

Fig. 6. Accuracy and precision statistics for Foretrex 401, Google Nexus 7 and HBT-LS.

Assuming normally distributed errors in the horizontal coordinates CMAS can be described mathematically as

$$CMAS = 2.1460\sigma_c \tag{12}$$

TABLE I
HERBICIDE DOSES (GRAMS OF ACID EQUIVALENT TARGET^{-1}) DERIVED FROM HBT-LS COMPARED TO COMPOSITE AVERAGES

Date	03/27	04/22	04/23	04/24	05/08	05/09	05/20
Targets[a]	142	97	49	40	2	13	37
Mean[b]	3.39	4.04	7.21	9.60	14.46	11.40	5.92
±SD[c]	2.40	2.80	6.26	7.34	4.37	1.39	3.58
Avg_{comp}[d]	3.68	3.95	6.86	8.84	17.55	12.27	7.02
Δ(%)[e]	8.0	2.4	5.0	8.2	19.3	7.4	16.9

[a] Number of targets treated during operation
[b] Mean herbicide dose derived from HBT-LS assignment to individual projectiles
[c] Standard deviation of herbicide dose derived from HBT-LS
[d] Average composite derived from the total number of pods consumed (~160 projectiles each) divided the total number of targets treated in each operation
[e] Percent difference between mean herbicide use determined based on HBT-LS usage statistics and average composite

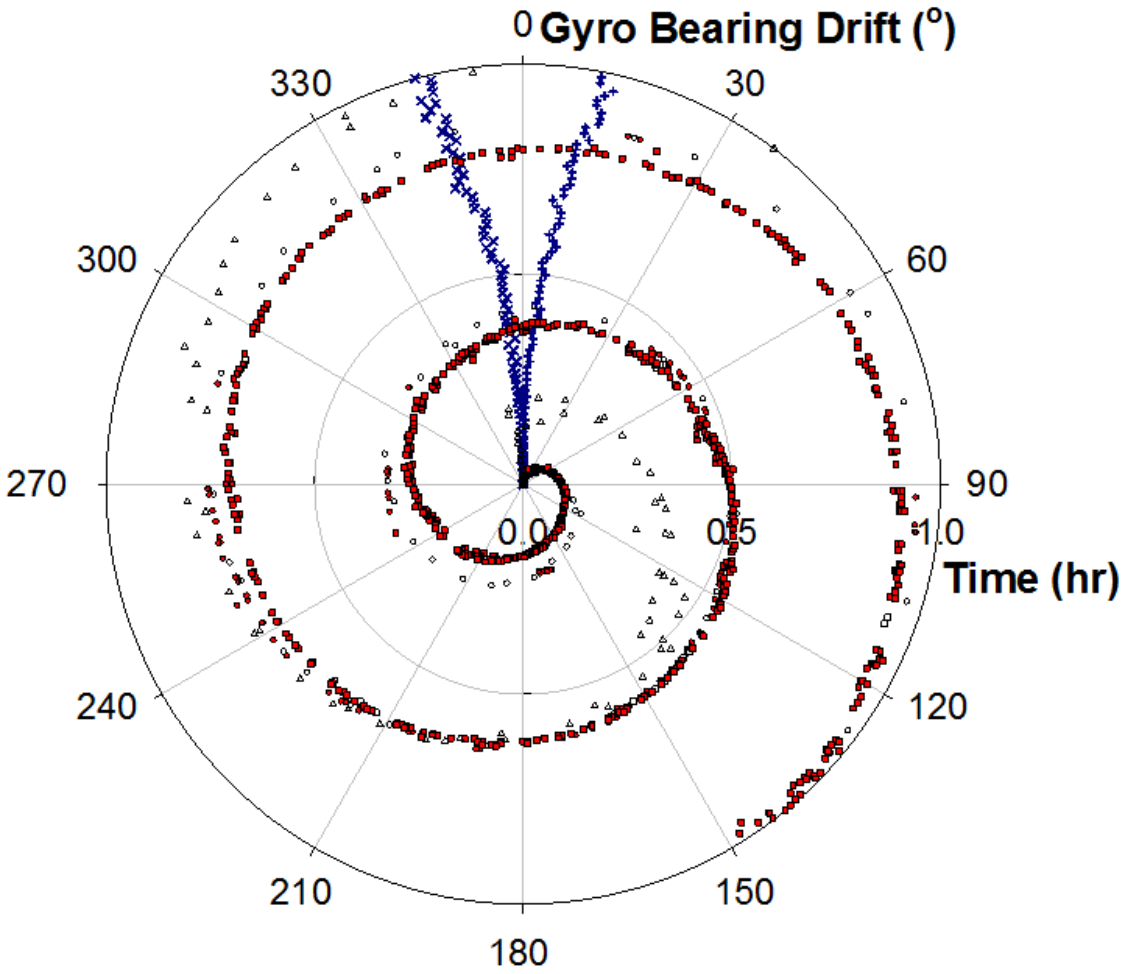

Fig. 7. Deviation in gyroscope bearing with respect to compass bearings (in degrees) over time, for stationary logger unit with sensor z axis (×) or y axis (+) aligned with vertical/gravitational force, or recorded under dynamic conditions over the course of three separate airborne operations (circles, squares, and triangles). Symbols without fill are trackpoint data during aerial operations, and red filled symbols are associated with projectile discharges. To remove clutter data was decimated leaving only every 10th data point.

where the circular standard error σ_c can be approximated by

$$\sigma_c \sim \frac{1}{2}\left(\sigma_x + \sigma_y\right) \tag{13}$$

where σ_x and σ_y are the standard deviations in horizontal position corresponding to errors in latitude and longitude, respectively, assuming that the larger of two is less than 5x the magnitude of the other [21].

Precision of a GPS receiver in three dimensions, including the z (vertical) direction, is given by the Spherical Accuracy Standard (SAS), which is defined as the magnitude of the radius of the smallest sphere containing 90% of the recorded positions. This value can be estimated as

$$SAS = 2.5\sigma_s \tag{14}$$

where σ_s is the spherical standard error approximated by

$$\sigma_s \sim \frac{1}{3}\left(\sigma_x+\sigma_y+\sigma_z\right) \quad (15)$$

where σ_z is the standard deviation in altitude, assuming that the smallest of the three component standard deviations is not less than 0.35x the magnitude of the largest [21].

On July 20, 2014, calibrations were performed with the HBT-LS and other consumer-grade GPS receivers against a GPS reference station (Trimble NetRS: 21° 17′ 50.46″ N, 157° 48′ 58.95″ W, 81.378m above sea level) located in Honolulu, HI. The consumer-grade GPS units calibrated in this study included a Google Nexus 7 tablet independent of the HBT-LS and the Foretrex 401 handheld (Garmin Olathe, KS). These GPS units were placed at the base of the reference station antenna on the roof and their positions recorded every 5 seconds for 3 hours. With the sensor board mounted to the marker, the HBT-LS was mounted in an articulated vise (PanaVise 350, Reno, NV) at a horizontal distance of approximately 18 meters from and aligned azimuth to target the reference position with azimuth 290°. In this attitude data was recorded by the HBT-LS every 5 seconds for 3 hours. Accuracy for all test receivers was determined by RMSE relative to the known reference position, while precision was determined by radial magnitudes for CMAS and SAS as described above. The reference position was estimated from HBT-LS data using the known distance to target to completely define the vector from marker to the reference.

V. Dynamic Accuracy and Precision in Operations

Aerial surveillance operations were conducted in 2014 targeting *Miconia calvescens* and *Psidium cattleianum* weed populations on Maui with the HBT-LS integrated to the electro-pneumatic marker. Operations were conducted using a Hughes 500D helicopter with the applicator positioned on the port side behind the pilot as described by Leary et al. [10]. In these operations, the HBT-LS recorded all projectiles discharged with timestamp and target assignment along with all other calibrated sensor information. Operational data were evaluated to determine the distribution of projectile trajectories with respect to the nose of the aircraft and the horizontal plane.

For a data subset (n = 362) an additional HBT-LS was positioned at the nose for calculation of the angle between the applicator and aircraft azimuths and bearing for comparison with the horizontal target window (i.e., 270° to 330°) corresponding to the shared view of the pilot and applicator. Tilt values were compared to the vertical target window (i.e., 0° to −50°). Altitude above ground level (Alt_{agl}) was estimated as the difference between the elevation inferred from the barometric pressure readings and the raster pixel value of the digital elevation model (DEM; 10m resolution) corresponding to the recorded point location.

Herbicide dose accuracy was measured as the percent difference between mean target dose rate recorded by HBT-LS (average number of projectiles used to treat each unique target ID) and composite averages in each operation estimated by dividing the total number of pods (projectile containers) consumed (∼160 projectiles per pod) by the total number of targets treated in an operation, with rounding errors expected [9].

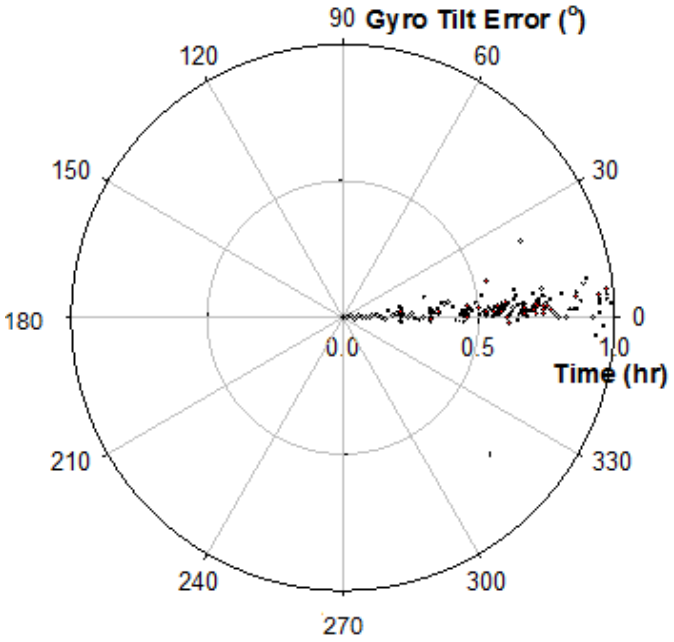

Fig. 8. Deviation in tilt estimate from gyro with respect to tilt estimate from compass, for data in a single aerial operation. Red filled symbols are data associated with a projectile discharge, and unfilled symbols are from trackpoint data. Data are decimated to show only every 10th data point to remove clutter.

VI. Results

A. Accuracy and Precision of Target Coordinates

Both HBT-LS and tablet exhibited static circular and spherical precisions about seven times smaller than the corresponding values recorded for the handheld GPS unit (Fig. 5). Accuracy (RMSE) of the tablet was also superior to the other GPS unit in 2D and 3D, while the HBT-LS was superior to the handheld GPS in 3D accuracy (Fig. 6). Moreover, it is worth noting how the BCM4751 receivers of the HBT-LS and tablet were coinciding with much more stable plots of the coordinates in the short three hour period compared to the widely dispersed random appearance of the handheld GPS (see Fig. 6). The HBT-LS points are shifted further from the reference point, which is likely due to compounding errors exhibited by the tilt and azimuth sensors used for determining the target location and approximations made in installation and offset calculation.

B. Operational Validation

The HBT-LS successfully acquired data from seven independent operations in 2014 for a total of 11,132 projectiles assigned to 400 targets. Android tablets never became disconnected, textual data displayed on the app was constantly refreshed during operations, and the system was never observed to miss a trigger pull during operation, suggesting that the data communication was robust. By assigning target IDs to each projectile with the HBT-LS, we were able to qualitatively identify the target dose outliers (i.e., a large target

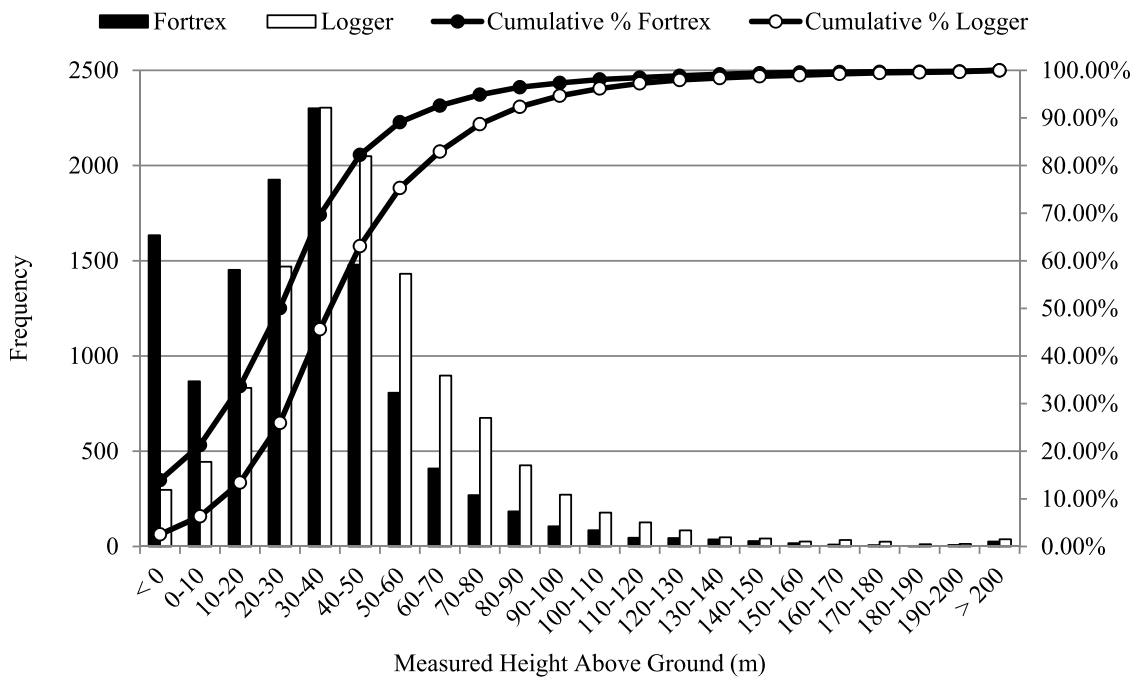

Fig. 9. Altitude above ground at the point of application estimated from elevation measurements from the HBT-LS (n = 11, 724) and Foretrex 401 (n = 11, 745) with ground level inferred from a 10-m digital elevation model at the recorded location.

treated with large projectile quantity) and also calculate mean values with standard deviations for each operation (Table I). In total, the HBT-LS mean (± standard deviation) calculations were within 11% of the composite estimated values. Anecdotally, herbicide dose corresponds to weed target size, so that HBT application data can be useful for assessing population age and phenology across the geographical range of operations. The standard deviations observed in this data set were rather large relative to the mean, suggesting diverse target populations. The capability of generating standard deviations will enhance interpretations with measures of uniformity and for segregating target outliers based on size class.

Efforts to determine the accuracy of the azimuth offset relative to the target window deduced from the track vector bearing were prone to large errors, particularly when the aircraft was in a stationary hover and pivoting on its axis (data not shown) such that the track direction did not coincide with the aircraft orientation. Despite a large interquartile range, the most frequent azimuth offset estimated for applicator relative to aircraft nose under these conditions was 311°. Vertical tilt estimates, on the other hand, were independent of aircraft bearing and so had a much tighter interquartile range of −20° to −41°. The more limited azimuth data subset relative to aircraft orientation recorded simultaneously by a separate logger in the cockpit displayed an interquartile range from 292° to 335°, contained within the perceived target window.

The average time on target (time interval between the first and last projectile discharged) was 12.3 ± 9.8 s.

To determine the stability of the gyroscope readings of azimuth and tilt (relative to those from the digital compass readings) were recorded both under static and dynamic conditions, and plotted against time (Figs. 7 and 8 respectively). Stationary data indicated that gyroscope readings have small axis-dependent biases in rotational velocity, which does not completely explain the relatively large systematic drift observed during aerial operations. Furthermore, the systematic drift experienced during aerial operations is not explained by random integration errors in the digital motion processor on the MPU-6050. This suggests that vibration or other motion artifacts might superimpose significant biases onto the rotational velocity measurements around the vertical axis, for example by inducing sympathetic vibrations in the gyroscope oscillators at odd harmonics. The deviation in tilt is not subject to this systematic drift, as the digital motion processor in the gyroscope chip corrects for drift in the tilt measurements based on acceleration (gravity) measurements in the different axes. No systematic drift was observed in stationary measurements of the digital compass. In addition, compass bearing to targets in operational data corresponded closely to expectations in that application is primarily against weed targets populating cliffsides, so that trajectories were more or less perpendicular to contours of terrain maps in the direction of increasing elevation. These data suggest that the aircraft did not significantly distort or shield local geomagnetic fields, and that at least in the areas of our operations there are little if any local distortions in the field.

The $\mathrm{Alt_{agl}}$ values (applicator elevation estimated from barometric pressure relative to ground surface elevation estimated for the corresponding GPS position on 10m digital elevation model) estimated from operational data recorded from the HBT-LS and consumer-grade GPS, were highly variable and included some negative values (Fig. 9). It should also be noted that some dramatic weather changes occurred during several of the operations which likely confounded many of the altimeter

estimates based on the calibrated barometric pressure at the start of operations and correspondingly contributed to errors in Alt_{agl}.

VII. Conclusion

The HBT-LS provided satisfactory accuracy and precision relative to consumer-grade handheld GPS units currently in use, enhanced data acquisition with new spatial and quantifiable attributes, while maintaining a low profile relative to the marker. Testing in an operational setting showed that results are consistent with anecdotal observation and expectations. Improvements in altimeter recordings may be necessary for better determination of offset locations to targets. Implementation of laser rangefinders to determine the range to the plant target and altitude will further improve the utility of the logger and enable direct estimation of target location without requiring knowledge of elevation and reference to digital elevation maps. Use of a single chip 9 axis sensor and additional sensor fusion between the accelerometer, gyroscope and magnetic compass for improved bearing determination should also be implemented. While this system was developed for use with the HBT platform, alternative applications include the use of marking agents to track the positions of plants and animals, including invasive species or livestock, surveying difficult to reach terrain, and spatial analysis of video and still imagery recorded by UAVs.

Acknowledgment

The authors would like to thank Dr. J. Foster and the Pacific GPS Facility for allowing use of their GPS reference station for accuracy and precision experiment.

References

[1] G. W. Cox, *Alien Species in North America and Hawaii*, 1st ed. Washington, DC, USA: Island Press, 1999.

[2] L. Loope and F. Kraus, "Preventing establishment and spread of invasive species: Current status and needs," in *Conservation of Hawaiian Forest Birds: Implications for Island Birds*, New Haven, CT, USA: Yale Univ. Press, 2009.

[3] L. Loope, F. Starr, and K. Starr, "Protecting endangered plant species from displacement by invasive plants on Maui, Hawaii," *Weed Technol.*, vol. 18, pp. 1472–1474, Dec. 2004.

[4] H. A. Mooney and J. A. Drake, "Ecology of biological invasions of North America and Hawaii," in *Ecological Studies: Analysis and Synthesis*. Berlin, Germany: Springer-Verlag, 1986.

[5] C. P. Stone and J. M. Scott, *Hawaii's Terrestrial Ecosystems: Preservation and Management*, 1st ed. Honolulu, HI, USA: Univ. Hawaii Press, 1985.

[6] C. P. Stone, C. W. Smith, and J. T. Tunison, *Alien Plant Invasions in Native Ecosystems of Hawaii: Management and Research*. Honolulu, HI, USA: Univ. Hawaii Press, 1992.

[7] D. B. Lindenmayer, C. R. Margules, and D. B. Botkin, "Indicators of biodiversity for ecologically sustainable forest management," *Conserv. Biol.*, vol. 14, no. 4, pp. 941–950, 2000.

[8] C. Kueffer and L. Loope, "Prevention, early detection and containment of invasive, nonnative plants in the Hawaiian Islands: Current efforts and needs," Dept. Botany, Univ. Hawaii at Manoa, Honolulu, HI, USA, Tech. Rep. 166, Aug. 2009.

[9] J. J. K. Leary, J. Gooding, J. Chapman, A. Radford, B. Mahnken, and L. J. Cox, "Calibration of an herbicide ballistic technology (HBT) helicopter platform targeting *Miconia calvescens* in Hawaii," *Invasive Plant Sci. Manage.*, vol. 6, no. 2, pp. 292–303, Jan. 2013.

[10] J. J. K. Leary *et al.*, "Reducing nascent miconia *(Miconia calvescens)* patches with an accelerated intervention strategy utilizing herbicide ballistic technology," *Invasive Plant Sci. Manage.*, vol. 7, no. 1, pp. 164–175, Jan. 2014.

[11] J. S. Jang and D. Liccardo, "Automation of small UAVs using a low cost MEMS sensor and embedded computing platform," in *Proc. IEEE/AIAA 25th Digital Avionics Syst. Conf.*, Oct. 2006, pp. 1–9.

[12] M. Steen, P. M. Schachtebeck, M. Kujawska, and P. Hecker, "Analysis and evaluation of MEMS INS/GNSS hybridization for commercial aircraft and business jets," in *Proc. IEEE/ION Position Location Navigat. Symp. (PLANS)*, May 2010, pp. 1264–1270.

[13] J. Kolecki and P. Kuras, "Low cost attitude and heading sensors in terrestrial photogrammetry—Calibration and testing," *Archiwum Fotogrametrii, Kartografii Teledetekcji*, vol. 22, pp. 249–260, 2011.

[14] G. Troni and L. L. Whitcomb, "Preliminary experimental evaluation of in-situ calibration methods for MEMS-based attitude sensors and Doppler sonars in underwater vehicle navigation," in *Proc. IEEE/OES Auto. Underwater Veh. (AUV)*, Sep. 2012, pp. 1–8.

[15] G. Robinson and I. Robinson, "The motion of an arbitrarily rotating spherical projectile and its application to ball games," *Phys. Scripta*, vol. 88, no. 1, p. 018101, Jul. 2013.

[16] B. L. Decker, "World Geodetic System 1984," Defense Mapping Agency Aerospace Center, St. Louis, Mo, USA, Accession No. ADA167570, Apr. 1986.

[17] T. Vincenty, "Direct and inverse solutions of geodesics on the ellipsoid with application of nested equations," *Surv. Rev.*, vol. 23, no. 176, pp. 88–93, 1975.

[18] Federal Geographic Data Committee, "National standard for spatial data accuracy (NSSDA)," Federal Geographic Data Committee, Washington, DC, USA, Tech. Rep. FGDC-STD-007.3-1998, 1998.

[19] *Information Technology—Spatial Data Transfer Standard*, ANSI-NCITS Standard 320:1998, Jun. 1998.

[20] *United States National Map Accuracy Standards*, U.S. Bureau Budget, Washington, DC, USA, 1947.

[21] C. R. Greenwalt and M. E. Shultz, *Principles of Error Theory and Cartographic Applications*. St. Louis, MO, USA: Aeronautical Chart and Information Center, 1965.

Roberto Rodriguez, III (M'14) received the B.S. degree in biological engineering from the University of Hawaii at Manoa, Honolulu, HI, USA, where he is currently pursuing the M.S. degree in biological engineering.

He has been a Research Assistant with the Department of Molecular Biosciences and Biological Engineering, University of Hawaii at Manoa, since 2013, and a member of the American Society of Agricultural and Biological Engineers since 2014. His current research interests include the use of remote sensing for environmental and medical applications.

Daniel M. Jenkins received the B.S. and M.Eng. degrees in agricultural and biological engineering from Cornell University, Ithaca, NY, USA, in 1995 and 1996, respectively, and the Ph.D. degree in biological and agricultural engineering from the University of California at Davis, Davis, CA, USA, in 2001.

He has been a faculty member with the Department of Molecular Biosciences and Bioengineering, University of Hawaii at Manoa, Honolulu, HI, USA, since 2002, a member of the American Society of Agricultural and Biological Engineers since 1998, and a member of the American Chemical Society since 2005. His primary interest is in molecular and other sensor systems for agricultural and environmental applications.

James J. K. Leary received the B.S. degree in horticulture with a minor in chemistry from Michigan State University, East Lansing, MI, USA, in 1996, and the M.S. degree in horticulture and the Ph.D. degree in molecular biosciences and biological engineering with a specialization in weed science and molecular ecology from the University of Hawaii at Manoa, Honolulu, HI, USA, in 1999 and 2006, respectively.

He has served as a faculty member with the Department of Natural Resources and Environmental Management, University of Hawaii at Manoa, since 2009, where he ranked as an Assistant Specialist with a research and extension split appointment. His interests are applied research in invasive plant species management.